



## Numerical Analysis Considering the Dynamic Installation Effects of Stone Column on Soft Clay Response

Saleh I. Rashwan<sup>1),2)\*</sup>, A.M. Nasr<sup>1)</sup>, W.R. Azzam<sup>1)</sup>

<sup>1)</sup> Department of Structure Engineering, Faculty of Engineering, Tanta University, Tanta, Egypt.

<sup>2)</sup> Civil Engineering Department, Faculty of Engineering, Horus University-Egypt, New Damietta 34517, Egypt.

\* Corresponding Author. E-Mails: [saleh1458@gmail.com](mailto:saleh1458@gmail.com); [saleh160449@f-eng.tanta.edu.eg](mailto:saleh160449@f-eng.tanta.edu.eg)

### ARTICLE INFO

#### Article History:

Received: 22/12/2024

Accepted: 28/4/2025

### ABSTRACT

This study investigates installing stone columns and their influence on the behaviour of soft clay, with a particular focus on both lateral and dynamic changes induced during the installation process, focusing on two distinct installation methods established on Cylindrical Cavity Expansion (CCE) in the Finite Element (FE): a traditional approach and a dynamic installation technique. Stone columns are commonly used to enhance soil properties, including increasing bearing capacity, reducing settlement, and improving overall soil stability. Through (FE) modeling, the research examines the changes in key factors, such as lateral stress and soil stiffness, which are key factors in soil reinforcement. In the traditional method, the lateral pressure coefficient  $K$  reached values up to 2.25 for the most significant expansion ratio, while the normalized stiffness improved by 2.3 times the initial value. These changes enhanced the bearing capacity within a localized zone of 1 to 3 times the column diameter ( $r/D$ ), diminishing the effects beyond this range. However, the dynamic method showed even more significant improvements, with  $K$  exceeding 3.4 and stiffness reaching over 3.2 times the initial value for the same expansion ratio. This method resulted in a more controlled build-up of lateral stress, extending the bearing capacity improvements to 6 times the column diameter. The results indicate that while both techniques strengthen the bearing capacity and stabilize the surrounding soil, the dynamic installation technique offers a more pronounced and extended effect, making it a superior choice for capturing the dynamic impact. The study provides valuable insights into stone column installation methods for geotechnical projects requiring dynamic implications.

**Keywords:** Finite element, Dynamic installation, PLAXIS 2D, Soil stiffness, Stone column.

### INTRODUCTION

Stone columns, also called granular columns, represent a highly cost-effective and widely utilized method in geotechnical engineering for improving the properties of soft soil deposits. These columns are particularly successful in improving the bearing capacity of the soil and managing both total and differential settlements, which are critical in the foundations of

structures, such as liquid storage tanks, embankments, and raft foundations. In addition to their foundational benefits, some stone columns, also referred to as granular columns, are highly cost-effective and enhance slope stability, accelerate consolidation processes, and mitigate the risk of soil liquefaction in seismic-prone or unstable areas ((Greenwood & Kirsch, 1984).

Extensive research has been devoted to understanding the behaviour and performance of stone

columns through various approaches, including theoretical modeling and laboratory testing (Sakr et al., 2022a, 2022b) and field studies (McCabe et al., 2009). These studies aimed to gain deeper insights into the mechanics of stone columns, optimize their design parameters, and assess their long-term effects on soil stability (Hadri et al., 2021; Hamzh et al., 2022; Han & Ye, 1992; Vitkar, 1978). This research contributes to the ongoing development and refinement of stone column techniques, helping engineers achieve more efficient designs and predictable performance in practical applications (Debats et al., 2003; Mitchell & Huber, 1985; Mitra & Chattopadhyay, 1999; Priebe, 1995).

In standard engineering practice, the strength and stiffness of the surrounding soil are generally expected to remain unchanged after the induction of stone columns (El Sawwaf et al., 2024; Priebe, 1976). The main improvement in earth conditions is attributed to the highly compacted material within the stone columns. Any additional enhancement in the surrounding soil's properties is typically viewed as an implicit safety margin rather than a design requirement. When designing vibro-replacement stone columns, the increased performance of the surrounding soil is not usually factored into the calculations, except for a moderate increase in stress levels, often based on assumptions related to the earth pressure at rest ( $K_0$ ) (McCabe et al., 2009). Design parameters, such as soil stiffness and shear strength, are usually determined based on pre-installation investigations and are not subjected to additional verification or testing after the columns have been installed (Basha et al., 2024; Mohamed et al., 2023; Sathish et al., 1997). Recent developments in the field have shifted attention toward understanding how installing vibro-replacement stone columns affects the surrounding ground. Most of the existing two-dimensional and three-dimensional numerical models studying the behaviour of stone columns assumed that the columns are "wished-in-place" (Kirsch, 2006; Mitra & Chattopadhyay, 1999; Ranjan & Rao, 1986; Yousfi et al., 2023). The wished-in-place method proposes that the installation process is idealized as if the columns were installed without disturbing the surrounding soil or altering its properties. This study demonstrates that dynamic installation methods, such as vibrations and soil displacement, used in stone column installation significantly influence the surrounding soil's mechanical properties, leading to spatial variations in

the stress regime. Unlike previous research that neglected the dynamic effects of installation, in this study, the findings highlight the magnitude of considering installation dynamic effects when designing stone column systems, as these dynamic effects can alter the mechanical properties of the stone columns' and the surrounding soil. The conclusions drawn from this study provide valuable insights into soil densification, soil stresses, and pore water pressure of stone columns' post-installation, offering guidance for more accurate and reliable design practices. Although stone columns have been widely studied, most existing research adopts the "wished-in-place" assumption, neglecting the dynamic effects induced during installation. Limited studies have examined how dynamic installation methods influence lateral stress, soil stiffness, and excess pore water pressures in the surrounding soil. Furthermore, there is a lack of systematic comparison between traditional and dynamic installation techniques in finite element simulations. Addressing this gap, the present study aims to model traditional and dynamic stone column installation methods, quantify their effects on soil improvement, and provide a deeper understanding of the spatial variations in stress and stiffness induced by installation dynamics.

## VALIDATION MODEL

The finite element program results were verified by comparing the load-settlement behaviour obtained in the model with the empirical findings from Narasimha Rao et al. (1992). Their study provided detailed insights into the load-bearing capacity and settlement response of stone columns in soft clay soils, offering a reliable benchmark for assessing model accuracy. The finite element analysis was evaluated for its ability to replicate Rao et al.'s observed trends in settlement reduction and bearing capacity improvement by simulating similar loading conditions and soil properties. The comparison confirms the model's reliability in capturing critical load-settlement behaviours, demonstrating its suitability for predicting the performance of stone column systems in soft soils. The hardening soil model was used to define the clay layer, and the Mohr-Coulomb model was used to define the stone column. The properties are selected as shown in Table 1, and the geometry and analysis of load settlement are shown in Figure (1),

**Table 1. Parameters for soil classification and basic properties (Ambily & Gandhi, 2007)**

Soil Parameter	Material model	$E_{ref}$	$C_{ref}$	$\phi$	$E_{50}^{ref}$	$E_{oed}^{ref}$	$E_{ur}^{ref}$	$\nu$	$\gamma$	$\gamma_{sat}$
Stone Column	MCM	45000	0	38	--	--	--	0.3	18.2	18.9
Clay	HS	--	20	--	1250	1250	6000	0.45	16.2	17.0
Unit	--	kN/m <sup>3</sup>	kN/m <sup>3</sup>	°	kN/m <sup>3</sup>	kN/m <sup>3</sup>	kN/m <sup>3</sup>	--	kN/m <sup>3</sup>	kN/m <sup>3</sup>

In this context, ( $E_{ref}$ ) is Young's modulus for stone column, ( $C_{ref}$ ) is soil cohesion, ( $\phi$ ) is friction angle, ( $E_{50}^{ref}$ ) is the reference secant stiffness modulus, ( $E_{oed}^{ref}$ ) is the reference oedometer modulus, ( $E_{ur}^{ref}$ ) is the reference unloading/reloading stiffness modulus, ( $\nu$ ) is Poisson's ratio, ( $\gamma$ ) is the soil unit weight and ( $\gamma_{sat}$ ) is saturated soil unit weight.

demonstrating the load-settlement curve and geometry of the validation model (Narasimha Rao et al., 1992),

### NUMERICAL MODELING

The methodological approach used in the current study can be described as the expansion of a cylindrical cavity that can serve as a simulation method to mimic the lateral expansion of a vibrating poker during the installation of columns in cohesive soil. This approach is convenient when combining the (CCE) with the Finite Element (FE) method (El Sawwaf et al., 2017).

#### Material Behavior Models in Finite Element Simulation

This study utilized two material behaviour models in (FE) simulation. The Hardening Soil Model (HSM) is used to simulate the mechanical behaviour of the soft soil layers (Azzam et al., 2024; El-Nemr et al., 2023; Sakr et al., 2022), effectively capturing the soil's non-linear response under different loading conditions. Meanwhile, the Mohr-Coulomb Model (MCM) was applied to define the stone column's material properties (Mohamed et al., 2023), providing a straightforward method for characterizing its strength and deformation behaviour. By integrating both models, the study aims to better understand the relations between the stone columns and the nearby soil, ultimately enhancing ground improvement design techniques.

where the results of the experimental work validate the PLAXIS model with a load-settlement curve.

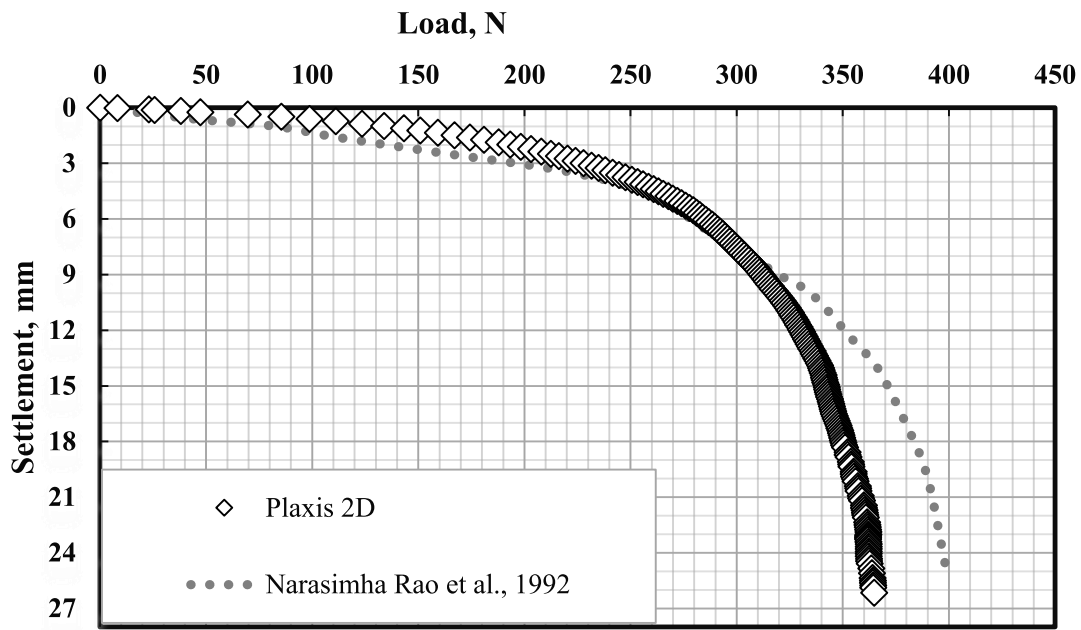
#### Cylindrical Cavity Expansion

While CCE may not precisely capture the vibrations caused by the poker or the step-by-step compaction of columns from the base upward, it remains a valuable approach for modeling the lateral expansion of a granular column into the surrounding soil. In practical applications, installing columns involves creating a void within the soil. Therefore, when using CCE to simulate column installation, the process should reflect the gradual expansion of a void from a first radius of zero to reach the final column radius.

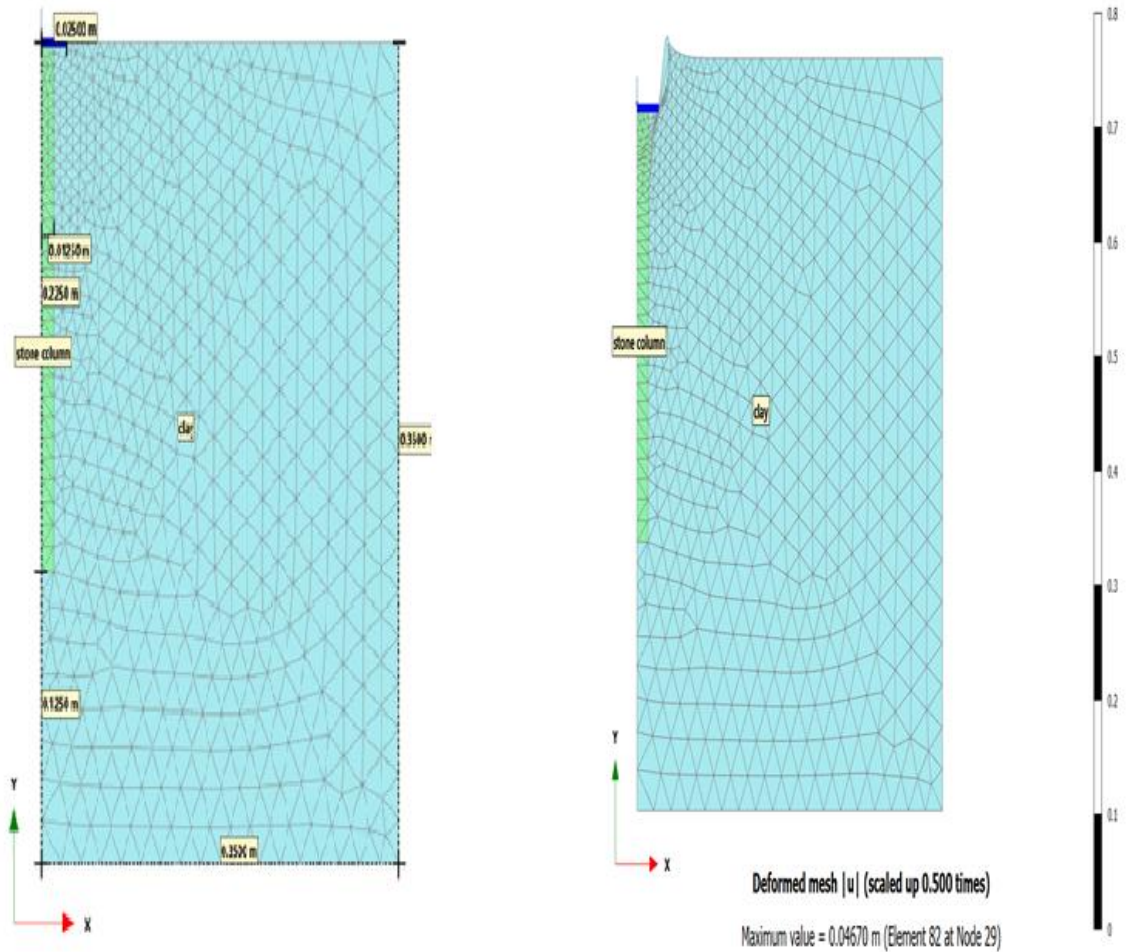
However, avoiding infinite circumferential strain in numerical simulations is important, since it potentially leads to unrealistic results. To ensure accuracy, the internal pressure within the void must reach a specific limit, known as " $P_{lim}$ ". Gibson and Anderson (1961) defined this limit pressure. Moreover, it is calculated using the following equation:

$$P_{lim} = P_o + C_u \left\{ 1 + \left[ \frac{E}{2c_u(1+\nu)} \right] \right\} \quad (1)$$

where  $P_o$  represents the original horizontal stress *in situ*,  $c_u$  is the undrained shear strength of the soil,  $E$  is the Young's modulus of the soil, and  $\nu$  is its Poisson's ratio, acting as a check against numerical inaccuracies, thus contributing to the overall reliability of the simulation.



A) load-settlement analysis of FE model for validation



B) FE geometry model for validation

C) Deformed mesh in PLAXIS 2D

Figure (1): A) load-settlement analysis of the FE model for validation. B) FE geometry model for validation. C) Deformed mesh in PLAXIS 2D (Narasimha Rao et al., 1992)

**Table 2. Parameters for soil classification and basic properties (Shehata et al., 2018)**

Soil Parameter	Material model	Depth	Material Behavior	OCR	$\gamma$	$\gamma_{sat}$
Platform & Stone Column	MCM	0.0-14.5	Drained	--	19.0	21.0
Crust	HS	0.0-1.5	Undrained	1.5	18.0	18.0
Upper Carse Clay	HS	1.5-2.5	Undrained	1.5	16.5	18.0
Lower Carse Clay	HS	2.5-14.5	Undrained	1	16.5	18.0
Unit	--	m	--	--	kN/m <sup>3</sup>	kN/m <sup>3</sup>

**Soil elasticity, strength, and permeability parameters (Shehata et al., 2018)**

Soil Parameter	$\nu$	$E_{ref}$	$C_{ref}$	$\phi$	$\psi$	$e_0$	$K_0$	$K_h$	$K_v$	$m$	$p_{ref}$
Platform & Stone Column	0.3	35000	0	38	6	--	1.0	1.5	1.5	--	--
Crust	0.35	--	3	34	0	1.0	1.5	$10^{-4}$	$6.9 \times 10^{-5}$	1.0	13
Upper Carse Clay	0.35	--	1	34	0	1.2	1.0	$10^{-4}$	$6.9 \times 10^{-5}$	1.0	20
Lower Carse Clay	0.35	--	1	34	0	2.0	0.75	$10^{-4}$	$6.9 \times 10^{-5}$	1.0	30
Unit	--	kN/m <sup>3</sup>	kN/m <sup>3</sup>	°	°			m/day	m/day		

**Parameters for clay soil stiffness and compression (Shehata et al., 2018)**

Soil Parameter	$E_{50}^{ref}$	$E_{oed}^{ref}$	$E_{ur}^{ref}$	$C_c$
Crust	1068	1068	5382	0.07
Upper Carse Clay	506	506	3036	0.25
Lower Carse Clay	231	231	1164	1.12
Unit	kN/m <sup>2</sup>	kN/m <sup>2</sup>	kN/m <sup>2</sup>	

where (OCR) is the over-consolidation ratio, ( $\nu$ ) is poisson's ratio, ( $E_{ref}$ ) is Young's modulus for stone column, ( $C_{ref}$ ) is soil cohesion, ( $\phi$ ) is friction angle, ( $\psi$ ) is dilatancy angle, ( $e_0$ ) is initial voids ratio, ( $K_0$ ) is lateral earth coefficient, ( $K_h$ ,  $K_v$ ) stand for the horizontal and vertical permeability, ( $m$ ) is the material constant, ( $p_{ref}$ ) is reference pressure, ( $E_{50}^{ref}$ ) is the reference secant stiffness modulus, ( $E_{oed}^{ref}$ ) is the reference oedometer modulus, ( $E_{ur}^{ref}$ ) is the reference unloading/reloading stiffness modulus, ( $C_c$ ) is the compression index, and ( $C_s$ ) is the swelling index.

**Bothkennar Soft Soil Profile**

The FE analysis used soil parameters obtained from the Bothkennar clay profile, which were identified through comprehensive geotechnical investigations. These parameters, including cohesion and friction, were essential for accurately modeling the soil's behaviour under various load conditions. The Bothkennar clay profile, derived from well-established geotechnical research from several studies, including the friction angle and cohesion values, was selected based on field and laboratory measurements reported by Fayed et al. (2018) and Nash et al. (1992). The relatively high friction angle ( $\Phi=38^\circ$ ) reflects drained strength conditions for stability analysis, while the low undrained cohesion captures the natural softness of the crust and upper Carse clay layers. The at-rest lateral pressure coefficient ( $K_0$ ) was assigned values consistent with over-consolidated behaviour, with  $K_0=1.5$  for OCR=1.5 layers, ensuring realistic initial stress states in the model. This study represents the soft soil surrounding the stone

columns. Comprehensive investigations conducted by (Hight et al. (1992), along with Fayed et al. (2018), and Nash et al. (1992) have provided detailed data on the properties of this clay. Table 2 presents the properties and soil classification, basic properties, soil elasticity, strength, permeability parameters, as well as clay soil stiffness and compression parameters.

**Adopted Numerical Modeling**

As shown in Figure (2), stone columns, the dimensions of which were selected based on (Al Ammari & Clarke, 2016; Fayed et al., 2018; Shehata et al., 2018), are installed rapidly, and their expansion process is considered to occur under undrained conditions due to quick installation. A numerical technique, called the "dummy material", is utilized (linearly elastic with an extremely low elastic modulus, typically around  $E = 20.0$  kPa). to simulate the presence of a void or weak remolded soil during the initial stages of installation. This technique facilitates numerical

stability and realistically represents the absence of structural support before the expansion and densification of the stone column. The poker is gradually inserted to reach the corresponding stone column depth, with water pumping applied as needed, and then subjected to horizontal vibrations. Initially, the hole for the column has a set radius ( $r_a$ ) and contains remoulded soil, known as “dummy material”, which

may change throughout the installation. Due to the horizontal vibrations from the poker, the hole's radius expands from the initial value ( $r_a$ ) to the stone column's final targeted radius ( $r_c$ ). The “prescribed displacement” in the (FE) is preferred to describe the horizontal displacement ( $r_0$ ) that occurs from the initial to the final radius, as shown in the mesh and model geometry.

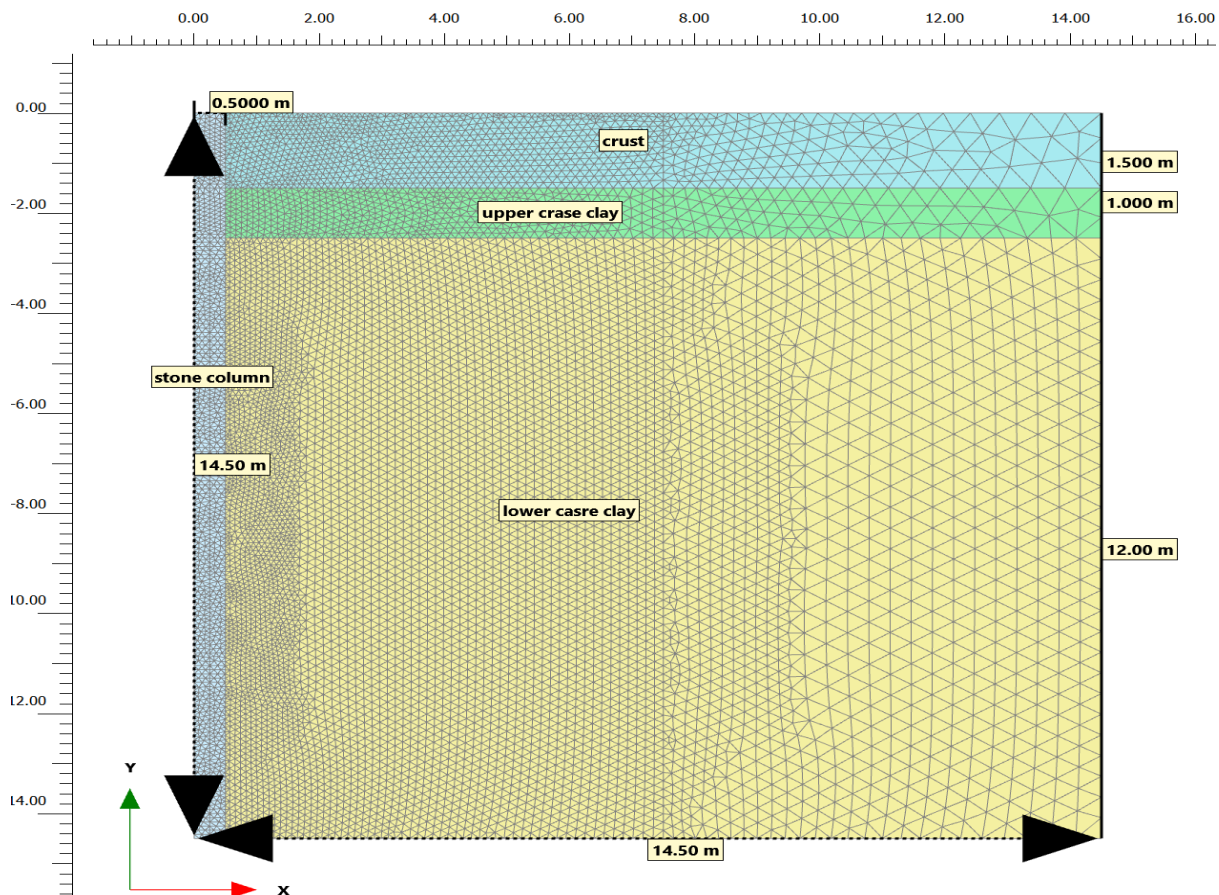


Figure (2): The (FE) and geometry model for the stone column

### The Traditional Scenario (First Case)

The simulation of column installation was carried out using PLAXIS 2D, and the cavity expansion method, which is the commonly used method for the simulation, has three key phases that follow the generation of initial stresses, achieved through the  $K_0$  procedure:

- a) The first phase models the cylindrical hole created using the poker, called a “dummy material” with a low Young's modulus. This “dummy material” represents the entire column length and extends radially to a distance labelled as  $r_a$ .
- b) Next, a pre-scribed displacement is applied along the

stone column height ( $L_c$ ), set at 14.5 meters under undrained conditions, to increase the radius from its initial value ( $r_a$ ) to the final radius ( $r_c$ ). A range of four lateral displacement values was evaluated ( $r_0 = 0.05, 0.15, 0.25, \text{ and } 0.35 \text{ m}$ ), each aligned with corresponding initial radius values ( $r_a = 0.45, 0.35, 0.25, \text{ and } 0.15 \text{ m}$ ). Once the poker is removed, the stone columns are assumed to have reached their final radius ( $r_c$ ).

- c) In the final phase, consolidation occurs to allow excess pore pressures to dissipate, solidifying the long-term stress changes in the ground caused by column installation.

Castro and Karstunen (2010) thoroughly detailed this approach, focusing on the broader stress redistribution and stiffness improvement associated with cavity expansion and dynamic installation methods. Interface elements with specified normal and shear stiffness could provide a more detailed interaction behaviour, which supports the validity of simplified contact assumptions for global response analysis (Castro & Karstunen, 2010). A pre-scribed displacement is the best option for ensuring numerical stability in the simulations.

**The Dynamic Scenario (Second Case)**

It was assumed that the dynamic effect of the poker moves concomitantly with the expansion process to capture the dynamic effect of the expansion imposed by the poker. Hence, the dynamic movement of the poker is considered throughout the expansion process. In PLAXIS 2D, using a cavity expansion technique, four distinct main phases follow initial stress generation, accomplished through the  $K_0$  procedure:

a) The initial step involves modeling the cylindrical

hole created by the poker using “dummy material” with a low Young's modulus. This “dummy material” extends the entire column length to a radial extent denoted as  $r_a$ .

- b) Afterwards, a pre-scribed displacement is applied to the height of the stone column ( $\Delta L_c$ ) under undrained conditions. In this case, ( $\Delta L_c$ ) equals a half of a meter, causing the radius to switch from the initial value,  $r_0$ , to the final radius,  $r_c$ . This displacement occurs at the stone column's base, utilizing the same five distinct lateral displacement values as in the first case.
- c) Subsequently, another pre-scribed displacement is applied to the subsequent one meter, and this sequential process continues until the entire 14.5-m stone column is completed.
- d) After the cavity expansion stage, a consolidation phase ensues to allow excess pore pressures to dissipate, establishing long-term stress changes in the ground induced by column installation, as shown in Figure (3).

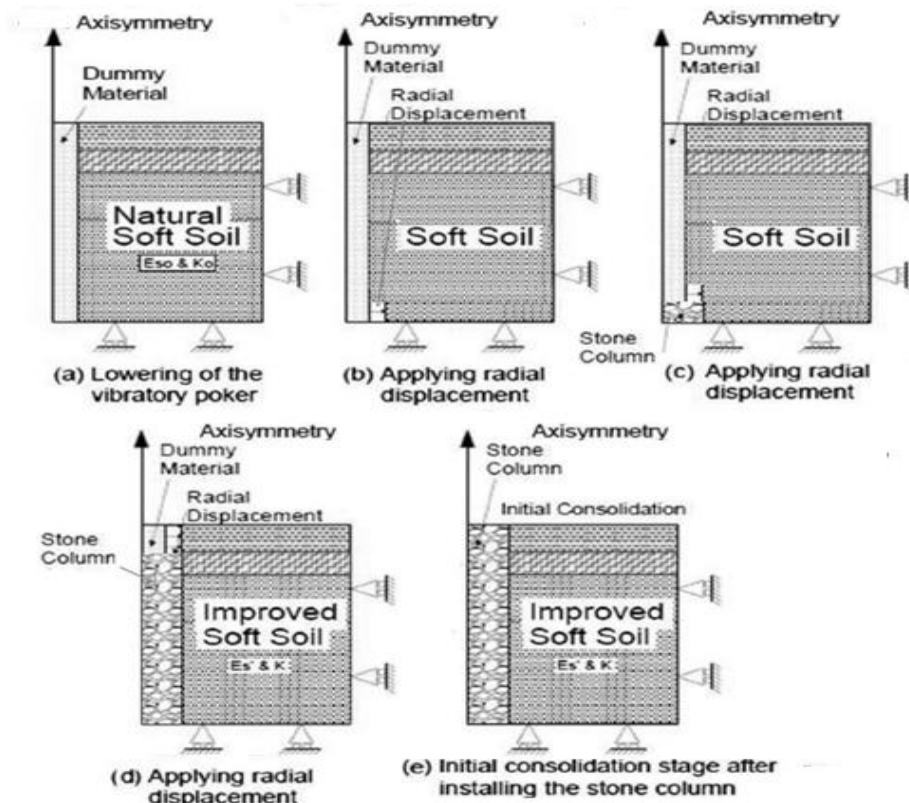


Figure (3): Installation stages for modeling a stone column for the second case

Following the consolidation phase and the resulting heightened horizontal stresses, it becomes feasible to calculate post-installation lateral earth pressure coefficients,  $K$ , using the following equation:

$$K = \frac{\sigma'_r}{\sigma'_v} \quad (2)$$

where  $\sigma'_r$  and  $\sigma'_v$  represent the effective radial and vertical stresses, respectively.

## RESULTS AND DISCUSSION

### Effective Improved Area

#### *The Traditional Scenario (First Case)*

The FE analysis results, taken immediately after the poker was removed and before the initial consolidation phase, indicate that the horizontal displacement contours show an impacted zone with a width of approximately eight times the diameter of the column. However, the displacement in the lower Carse clay appears relatively consistent across the depth of the clay layer, whereas the upper soil layers exhibit more irregular displacement patterns. The relative displacements ( $U_x/D$ , where  $U_x$  represents the radial movement of the clay soil) are depicted in Figure (4A) for the four expansion ratios analyzed at the near mid-depth of the clay layer (8.75 meters below the surface) to adjust the displacement data for consistency. For the case where  $r_0 = 0.25$  m, lateral soil movement is significantly higher close to the stone column, extending about 15% of  $D$  at a 1-meter distance from the column's centreline before rapidly decreasing. At 3 meters from the column's centre, the lateral displacement is around 5% of ( $D$ ). Similar patterns, with different magnitudes of horizontal displacement, are shown in Figure (4A) for the other radial expansion values ( $r_0 = 0.05, 0.15, 0.25,$  and  $0.35$  m). The analysis indicates that the installation process notably affects lateral soil displacement and compaction within an area extending from 1 to 3 times the stone column diameter. Beyond this range, horizontal movement and compaction gradually reduce, with minimal effects detected between 4 and 8.5 times the column diameter. The process's influence becomes negligible after 8.5 times  $D$  from the column's centreline.

#### *The Dynamic Scenario (Second Case)*

The FE analysis results for both cases reveal a similar overall pattern of lateral displacement and

compaction, with key distinctions in the extent of the affected zones. In both cases, the horizontal displacement contours illustrate a significant influence of the installation performance on the nearby soft soil. For the first case, the affected zone extends approximately 8 times the column diameter ( $D$ ), with notable lateral movement reaching around 20% of  $D$  at 1 meter from the column's centreline and gradually diminishing to about 10% at 3 meters. Beyond this range, the influence weakens, becoming negligible by a distance of 8 times  $D$ , the same as in the first case; in contrast to Figure (4B). The second case demonstrates that the installation's impact remains significant up to 4 meters from the column's centreline, after which the lateral displacements diminish more rapidly. By a distance of 6.5 times  $D$ , the effect of the installation becomes almost negligible. Despite these differences in the extent of the affected zone, both cases indicate that the installation process primarily affects a region within 1 to 3 times the column diameter, where lateral movements plus soil compaction are the most pronounced events.

### The Effective Lateral Stress Coefficient ( $K$ )

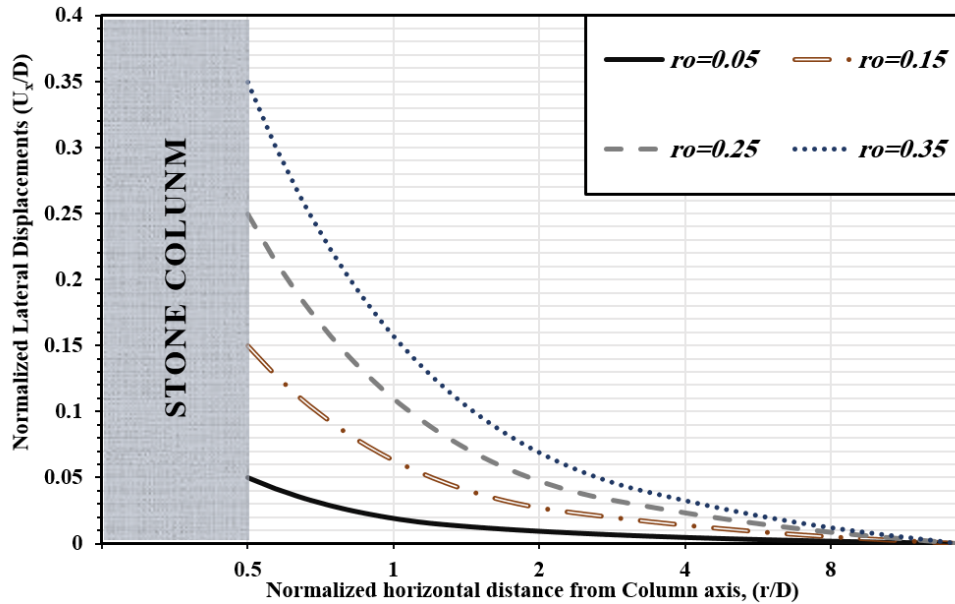
The coefficient of lateral earth pressure  $K$ , defined as the ratio of the effective horizontal stress ( $\sigma'_r$ ) to the effective vertical stress ( $\sigma'_a$ ), was analyzed after a 60-day consolidation period following stone column installation. The changes in  $K$  concerning ( $r/D$ ) are presented in the corresponding figures, covering the different radial expansions ( $r_0$ ) ranging from 0.05 to 0.35 meter (Sexton & McCabe, 2015).

#### *The Traditional Scenario (First Case)*

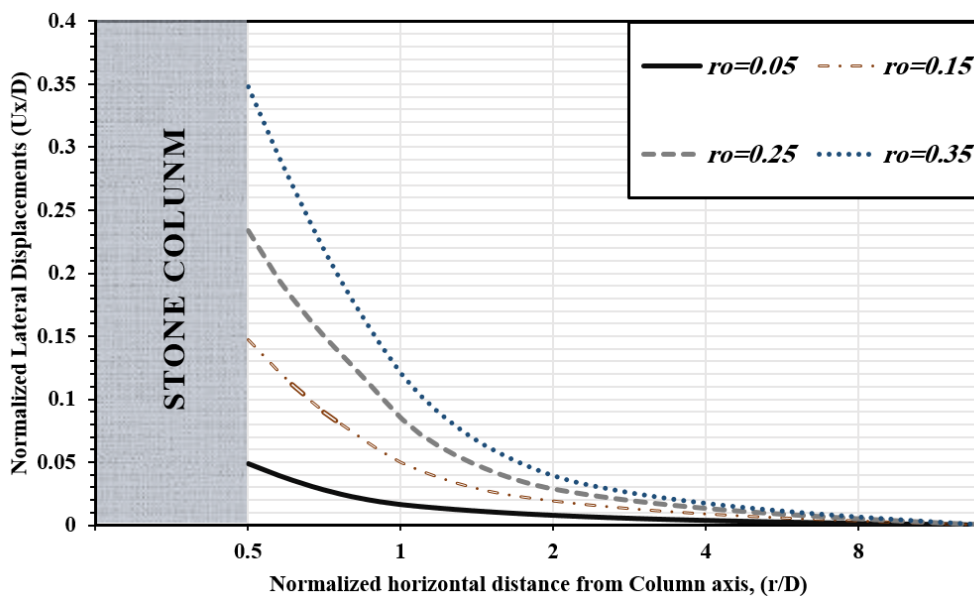
In this case, as shown in Figure (5A), the installation method significantly improved the lateral earth pressure coefficient ( $K$ ) near the stone column. For the most significant expansion ratio ( $r_0=0.35$ ), the lateral pressure values reached around 2.25 near the column axis. This pressure decayed quickly, becoming negligible beyond approximately ( $r/D = 6$ ). Smaller expansion ratios, such as ( $r_0=0.05$ ), exhibited lower lateral pressure values, with  $K$  reaching approximately 1.6 near the column, also following a similar pattern of rapid decay with distance. When examining the normalized lateral pressure ratio ( $K/K_0$ ) in Figure (5B), the trend was consistent for  $r_0=0.35$ , and the  $K/K_0$  ratio reached a value as high as 3.2 near the column, indicating that lateral pressures are

more than tripled compared to the initial at-rest condition. This ratio dropped rapidly with distance, stabilizing around  $K/K_0=1$  at approx.  $(r/D \approx 6)$ , where the effects of the installation became negligible. For smaller expansion ratios ( $r_0=0.05$ ), the  $K/K_0$  values were closer to 1.8 near the column, demonstrating how the radial

expansion affected the lateral pressure. This case highlights that while larger expansion ratios lead to higher lateral stresses, the overall behaviour shows a consistent decrease in pressure beyond 6-8 times the column diameter, confirming the localized effect of the installation.

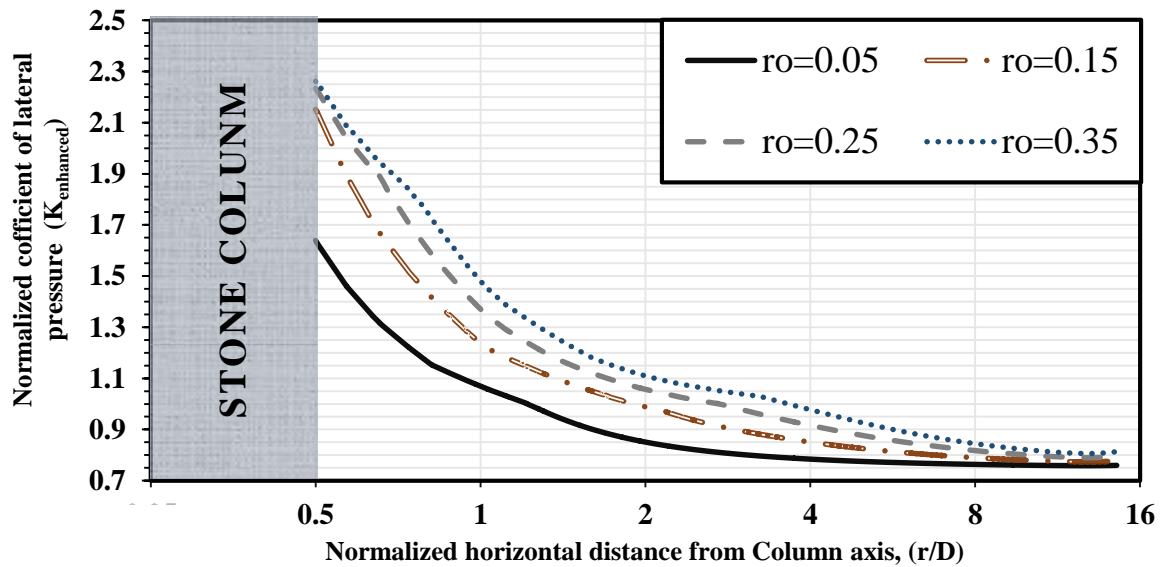


A) The normalized lateral displacement ( $U_x/D$ ) distribution of horizontal displacements for the traditional scenario based on Shehata et al. (2018) for different expansion ratios ( $r_0$ )

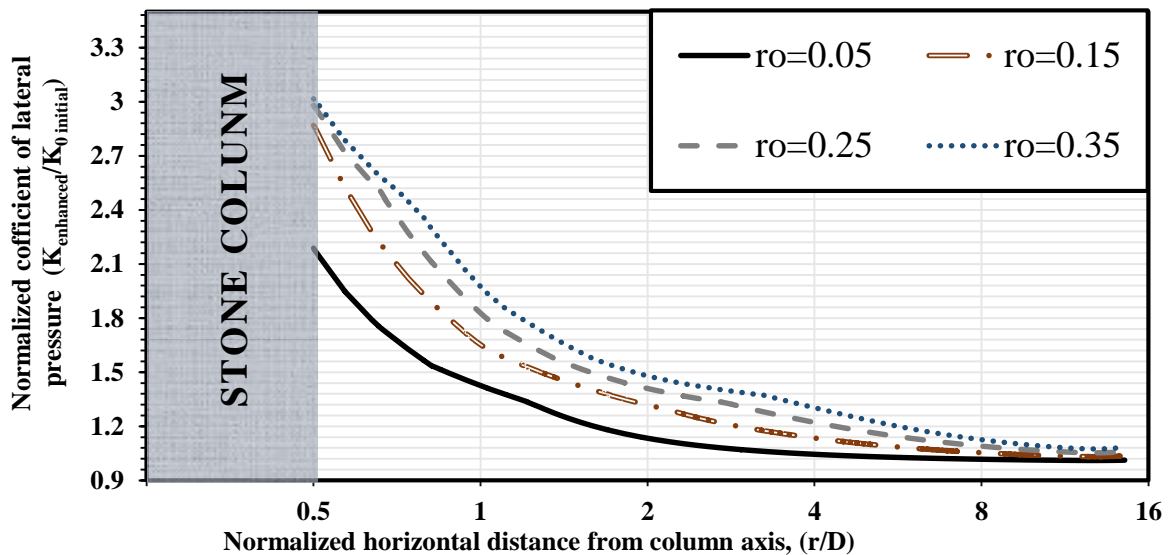


B) The lateral earth pressure ratio ( $K/K_0$ ) plotted against the radial distance for different expansion ratios ( $r_0$ )

**Figure (4): Normalized distribution of lateral displacement ( $U_x/D$ ) versus normalized radial distance ( $r/D$ ) for different expansion ratios ( $r_0$ ). A) The traditional scenario based on Shehata et al. (2018) at a vertical distance of 8.75 meters. B) The dynamic scenario**



A) The lateral earth pressure coefficient (K) plotted against the radial distance based on Shehata et al. (2018) for different expansion ratios ( $r_0$ )



B) The lateral earth pressure ratio ( $K/K_0$ ) plotted against the radial distance for different expansion ratios ( $r_0$ )

**Figure (5): A) The lateral earth pressure coefficient (K) plotted against the radial distance.  
B) The lateral earth pressure ratio ( $K/K_0$ ) plotted against the radial distance.  
Both are at 8.75m from the surface of the column for the first cases of  
horizontal different expansion ratios ( $r_0$ )**

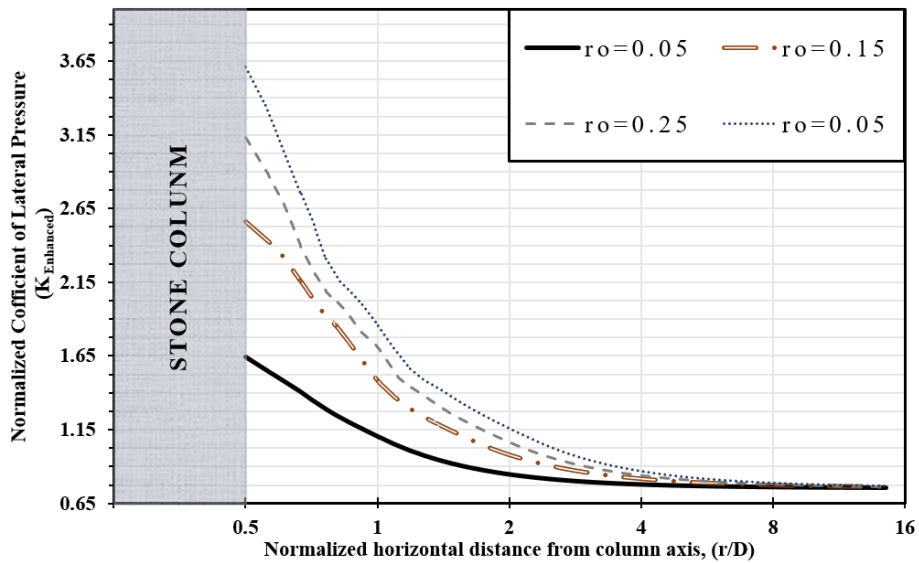
**The Dynamic Scenario (Second Case)**

In this case, as illustrated in Figure (6 A), a stone column was installed using a dynamic method, which involved dividing the installation into vertical steps of 0.5 meter each to achieve a total column depth of 14.5 meters. This method differs from the traditional approach by incrementally applying the installation forces, resulting in a more gradual build-up of lateral

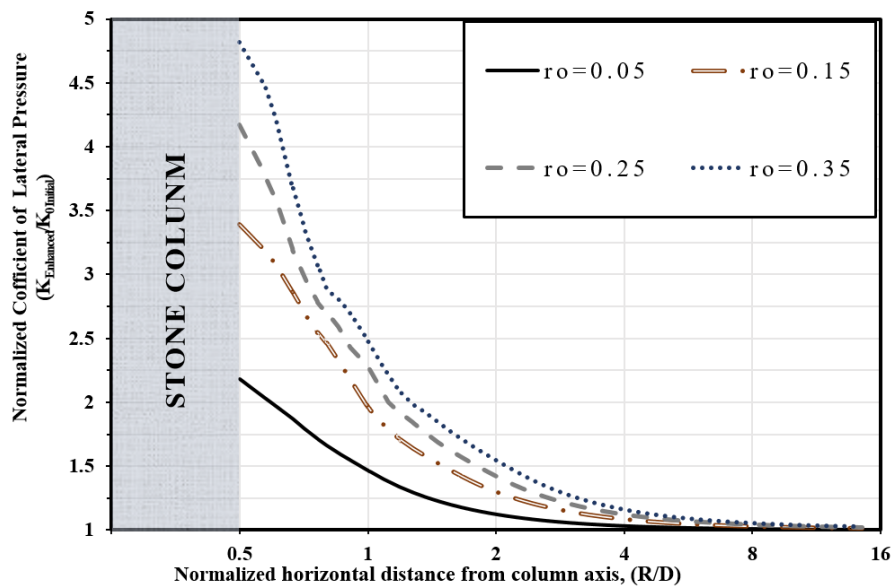
stresses. The dynamic installation produced significantly higher lateral pressure coefficients, especially near the column, compared to the first scenario. For the most significant expansion ratio ( $r_0=0.35$ ), (K) reached a value exceeding 3.4 near the column axis, showing a pronounced stress concentration in the soil surrounding the column. As the space from the column increased, the pressure decayed more

quickly than in the first case, becoming negligible at approximately  $r/D=6$ . This rapid decay suggests that while the near-field effects are more intense, the overall zone of influence may be slightly smaller. For smaller expansion ratios ( $r_0=0.05$ ), the lateral pressure was also higher in the near field compared to the first case, with values reaching around 1.8 near the column axis but quickly diminishing with distance. When considering Figure (6 B), the dynamic method caused a more significant increase, especially for higher expansion ratios. For  $r_0=0.35$ , the  $K/K_0$  ratio reached over 4.5,

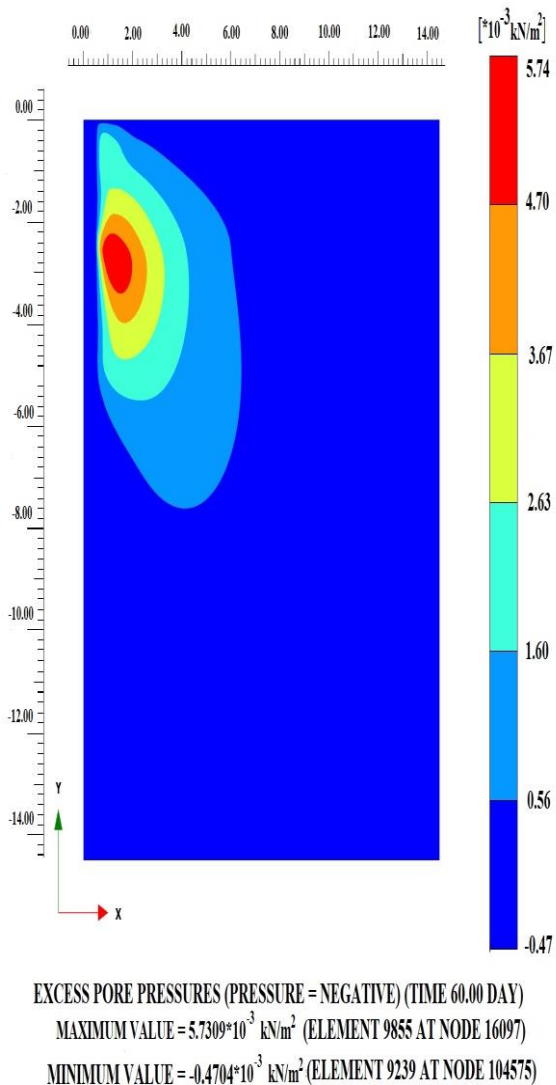
indicating that the dynamic method had a more concentrated effect on increasing lateral stress near the column compared to the conventional method. This stepwise application of pressure allowed for better control of stress distribution, but also led to more pronounced local effects, especially for larger expansion ratios. Similar to the first case, the pressure diminished with distance, stabilizing beyond  $r/D=6$ , but the initial increase in lateral pressure was significantly more enormous, reflecting the unique characteristics of the dynamic method.



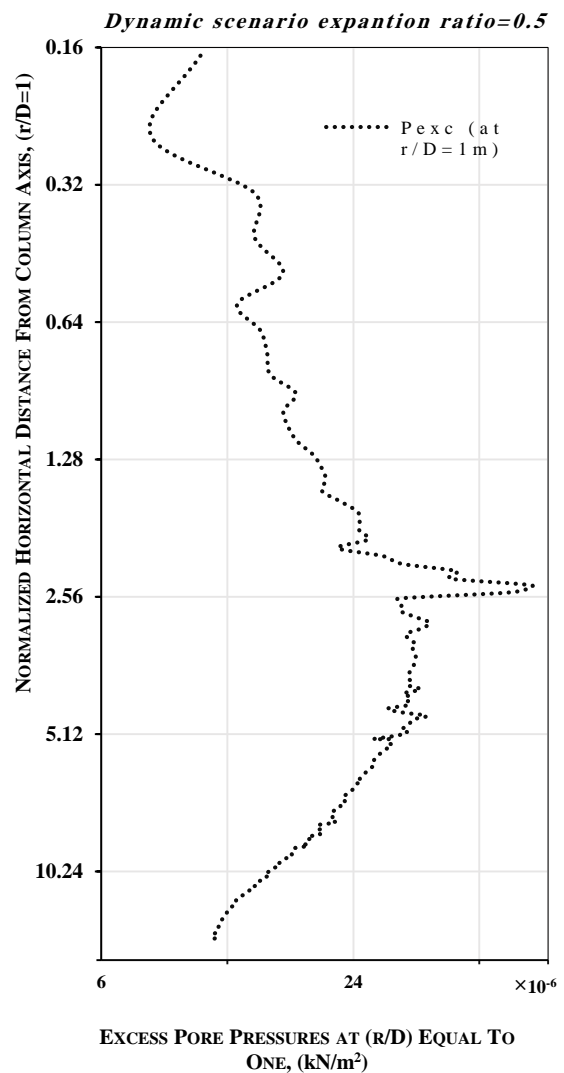
A) The enhanced lateral earth pressure ( $K$ ) trends for different expansion ratios ( $r_0$ ) at the level of 8.75m for the dynamic scenario



B) The normalized lateral earth pressure ( $K/K_0$ ) trends for different expansion ratios ( $r_0$ ) at the level of 8.75m for the dynamic scenario for different expansion ratios ( $r_0$ )



C) The excess water pore pressure  $P_{\text{excess}}$  for an expansion of  $r_0 = 0.25$  m after the consolidation phase shown for clay layers for the dynamic scenario



D) The excess water pore pressure  $P_{\text{excess}}$  for an expansion of  $r_0 = 0.25$  m at  $r/D=1$

**Figure (6): The soil lateral earth pressure and water pore pressure trend after the consolidation phase. A) The enhanced lateral earth pressure (K). B) The enhanced ratio of lateral earth pressure ( $K/K_0$ ). C) The excess water pore pressure  $P_{\text{excess}}$  for an expansion of  $r_0 = 0.25$ m. D) The excess water pore pressure  $P_{\text{excess}}$  at  $r/D=1$**

**The Excess Pore Pressure Distribution for the Dynamic Installation Method**

The consolidation and dissipation of excess pore pressures are essential for assessing the soil's long-term stability and settlement behaviour. In this case, the remaining excess pore pressures after 60 days indicate that the soil is still consolidating, which suggests that additional time may be needed for complete dissipation depending on soil permeability. The excess pore pressure distribution in the second case, as shown in Figure (6 C),

demonstrates the localized effects of the dynamic installation method. The plot highlights how the generated excess pore pressure responds to the lateral expansion and compaction induced by the installation process. As the stone column is installed, the surrounding soil is compressed, forcing pore water out of the saturated soil and creating this pressure build-up. This indicates that over time, this excess pore pressure would dissipate through consolidation, stabilizing the effective stresses in the soil. Understanding the distribution of excess pore

water pressure is crucial for evaluating the short-term stability after installation and the long-term behaviour of the improved soil. High pore pressures around the column initially reduce the effective stress, which can affect the stone column's immediate load-bearing capacity. As these pressures dissipate, the effective stress increases, improving the column's performance.

The dynamic installation method results in more concentrated excess pore pressures in the near-field zone, suggesting a more pronounced impact on pore water movement immediately around the column. The asymmetry in the pressure distribution may be due to boundary effects or specific model constraints. This non-uniform distribution could influence the direction and rate of consolidation, potentially impacting the column's load-bearing capacity. Over time, these pressures are expected to dissipate, improving the overall soil strength near the column. This pattern of pore pressure distribution supports the earlier findings of significant stress increases near the column, with effects tapering off at greater distances.

#### **Improved Stiffness (E)**

In this research, variations in soil stiffness are represented by the enhanced stiffness parameter ratio ( $E_{enhanced}/E_{initial} = E/E_0$ ), which is the ratio of the soil's enhanced stiffness post-installation to its initial stiffness before any modification. This parameter is a key indicator of the soil's response to loading and densification in the nearby area of the stone column due to the installation process. Analyzing this ratio quantifies how much the stone column installation improves the soil's ability to resist deformation. Biarez et al. (1998) introduced a specific formula, shown in Equation (3), to estimate the enhanced soil stiffness ( $E/E_0$ ) based on the variation in mean effective stress ( $p'/p'_0$ ), where  $p'$  represents the effective mean stress after construction, and  $p'_0$  denotes the initial effective mean stress. This equation is grounded in elastic-perfectly plastic theory and was initially developed using pressuremeter test results. Later, Brinkgreve and Broere (2006) suggested using  $m=1$  for soft clay soils, while Brinkgreve and Vermeer (1997) recommended employing the secant modulus ( $E = E_{50}$ ) as a reference value for usually consolidated clays. In this case, it corresponds to the stiffness modulus at 50% of maximum stress, which provides a more accurate depiction of soil behaviour under typical loading conditions.

$$E_{50\text{enhanced}}/E_{50\text{initial}} = \left(\frac{p'}{p'_0}\right)^m \quad (3)$$

In this scenario,  $E_{50}$  indicates Young's modulus,  $p'$  refers to the effective mean stress post-installation, and  $p'_0$  represents the effective mean stress preceding the installation.

$$p' = \frac{\sigma'_v + 2\sigma'_a}{3} \quad (4)$$

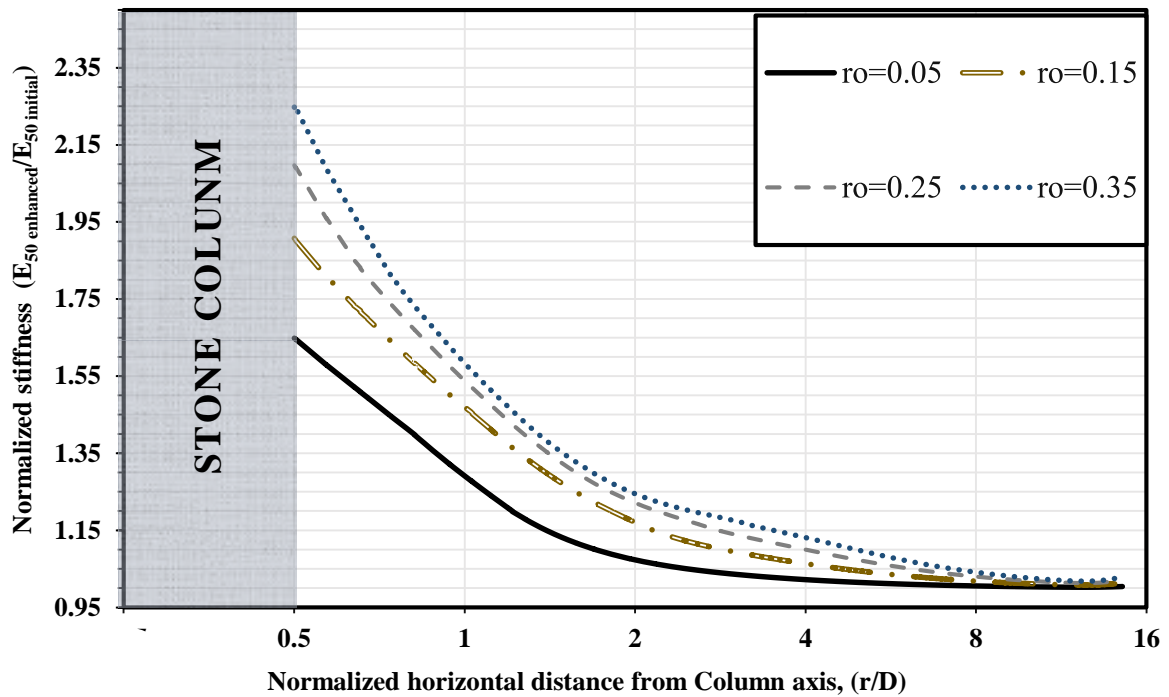
In these conditions,  $\sigma'_v$  corresponds to the effective vertical stress, and  $\sigma'_a$  denotes the effective radial stress.

#### **The Stiffness for Cases (Enhanced/ $E_0$ )**

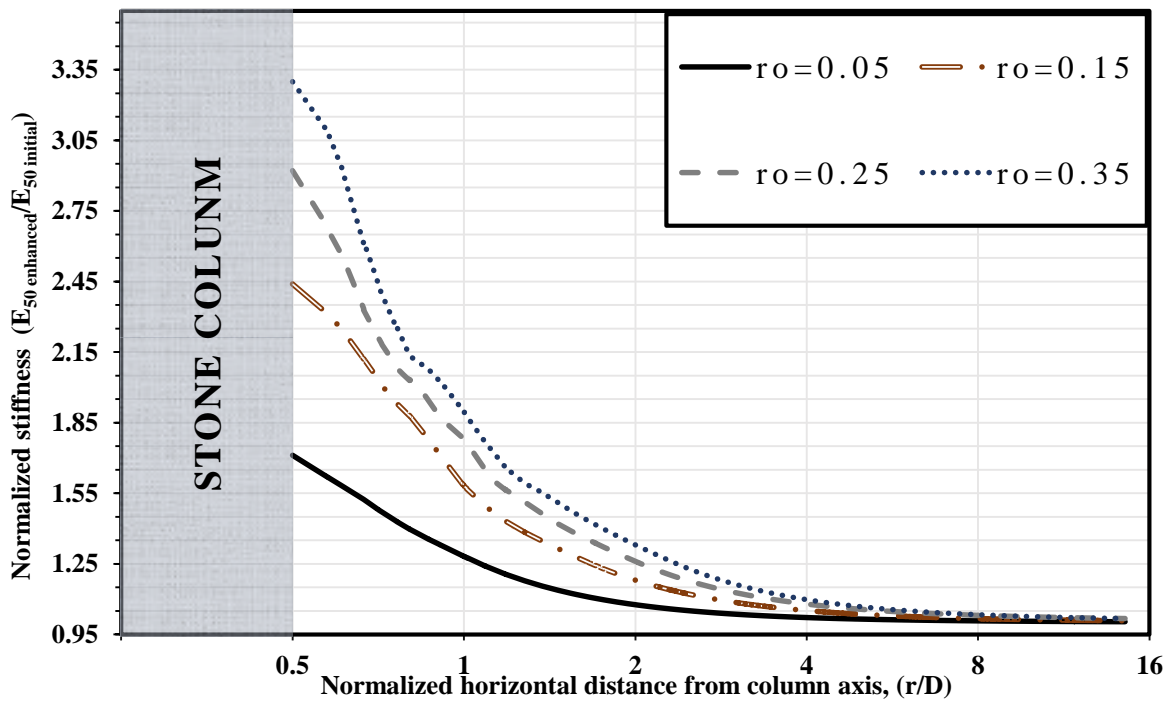
As shown in Figure (7), the second installation method led to significant improvements in soil stiffness near the stone column, particularly for larger radial expansion ratios. The graph shows that all expansion ratios have the highest normalized stiffness near the stone column ( $r/D \approx 1$ ). The most significant expansion ratio ( $r_0=0.35$ ) has the highest stiffness values, reaching over 3.2 times the initial stiffness in this case, which is more than in the first case, amounting only to 2.3 times the initial stiffness value for the same expansion ratio. This indicates that the soil near the column undergoes significant stiffness improvement due to the installation process. As the distance from the column increases, the stiffness decreases rapidly. When the distance reaches approximately 2-3 times the column diameter ( $r/D = 2-3$ ), the stiffness values for all expansion ratios start converging, indicating the diminishing impact of installing the stone column on soil stiffness.

For smaller expansion ratios like  $r_0=0.05$ , the increase in stiffness is relatively modest, with the value peaking around 1.7 near the column, which is the same as the first case scenario. However, for higher expansion ratios, the enhancement in stiffness is much more pronounced, especially near the column, which highlights the significant role that radial expansion plays in improving soil behaviour.

This impact decreases rapidly with distance from the column, becoming negligible beyond approximately 6 times the column diameter, where the stiffness returns to near its initial value. The dynamic installation method effectively increases the stiffness and densification in the near-field zone, enhancing the soil's load-bearing capacity and being denser around the column.



A) The enhanced stiffness parameter ( $E_{50\text{enhanced}}/E_{50\text{initial}}$ ) shown for the traditional scenario based on Shehata et al. (2018) for different expansion ratios ( $r_0$ )



B) The enhanced stiffness parameter ( $E_{50\text{enhanced}}/E_{50\text{initial}}$ ) is shown for The Dynamic Scenario for different expansion ratios ( $r_0$ )

**Figure (7): The enhanced stiffness parameter ( $E_{50\text{enhanced}}/E_{50\text{initial}}$ ) shown for different expansion ratios ( $r_0$ ) at a level of 8.75m for A) The traditional scenario based on Shehata et al. (2018), B) The dynamic scenario**

## CONCLUSIONS

This study investigated the effects of installing a stone column on the soil nearby, concentrating on two different installation methods: a traditional approach and a dynamic installation method. The findings demonstrate that stone column installation significantly improves the bearing capacity of soft soil by increasing both lateral stress and soil stiffness. However, the degree of improvement varies depending on the installation technique and the expansion ratio used.

In the first case, which followed a traditional installation method, the results show that the installation produced a noticeable increase in lateral stress and soil stiffness, particularly near the column. The lateral pressure coefficient  $K$  reached 2.25 for the most significant expansion ratio  $r_0=0.35$ , while the normalized soil stiffness ( $E_{\text{enhanced}}/E_0$ ) improved by 2.3 times the initial stiffness. These changes led to a significant enhancement in the bearing capacity within a localized zone, extending approximately 1 to 3 times the column diameter. However, beyond this distance, the installation's effects diminished, and the soil's bearing capacity returned to near its initial condition at a distance of 6 to 8 times the column diameter.

The lateral stress and soil stiffness improvements were more substantial in the second case, which utilized a dynamic installation method. The lateral pressure coefficient  $K$  reached values exceeding 3.4 near the column, and the soil stiffness improved by more than 3.2 times for  $r_0 = 0.35$ . The dynamic method resulted in a more controlled and gradual build-up of stress, leading to a more significant enhancement in load-bearing capacity compared to the first case. Additionally, the improved bearing capacity extended slightly farther from the column, with the effects remaining significant up to a distance of 6 times the column diameter before becoming negligible. The findings of this study align with previous research on stone column performance, with notable consistency in lateral stress enhancement within 2-3 times the column diameter, as observed by Castro and Karstunen (2010) and McCabe et al. (2009),

which also matches the range observed for the traditional installation method. Shehata et al. (2018) similarly reported lateral pressure coefficients near 2.5, which corresponds to the traditional scenario results in this study. However, the dynamic installation method demonstrated higher lateral stress ( $K > 3.4$ ) and greater stiffness improvement, emphasizing the additional effects of dynamic expansion that have not been extensively quantified in prior studies. This study highlights the importance of considering installation dynamics in future design practices. Overall, the dynamic installation method was more effective in increasing the bearing capacity of the surrounding soil, particularly in the near-field zone, producing higher lateral stresses and more significant stiffness improvements. While the present finite element study provides valuable insights into the effects of traditional and dynamic stone column installation, certain limitations should be acknowledged. The model assumes axisymmetric cylindrical expansion, idealized boundary conditions, and simplified soil-column interaction without explicit interface elements. Additionally, the simulations assume undrained conditions during installation without accounting for partial consolidation effects. While necessary for numerical feasibility, these assumptions may introduce deviations from complex field behaviour. Future studies could incorporate more advanced 3D modeling, interface formulations, and staged consolidation analysis to refine the results further. This would be more suitable for projects requiring enhanced soil stability and load-bearing performance. Although both methods improved bearing capacity, the dynamic method offered a more substantial and lasting effect, making it a promising option for soil reinforcement in soft clay environments. Future research should investigate variations in expansion ratios, installation methods, and the long-term behaviour of improved soil under different loading conditions to optimize stone column performance across diverse soil types and geotechnical applications.

## REFERENCES

- Al Ammari, K., and Clarke, B.G. (2016). "Predicting the effect of vibro stone column installation on performance of reinforced foundations". *International Journal of Civil, Environmental, Structural, Construction and Architectural Engineering*, 10 (2), 111-117.
- Ambily, A.P., and Gandhi, S.R. (2007). "Behavior of stone columns based on experimental and FEM analysis". *Journal of Geotechnical and Geoenvironmental Engineering*, 133 (4), 405-415. [https://doi.org/10.1061/\(ASCE\)1090-0241\(2007\)133:4\(405\)](https://doi.org/10.1061/(ASCE)1090-0241(2007)133:4(405))
- Azzam, W.R., Nasr, A.M., and Abdallah, S.S. (2024). "Geotechnical performance of XCC pile under torsion loads in clay soil: Numerical study". <https://doi.org/10.21203/rs.3.rs-4170200/v1>
- Basha, A., Azzam, W., and Elsiragy, M. (2024). "Utilization of sand cushion for stabilization of peat layer considering dynamic response of compaction". *Civil Engineering Journal (Iran)*, 10 (4), 1182-1195. <https://doi.org/10.28991/CEJ-2024-010-04-011>
- Biarez, J., Favre, J. L., and Hachi, F. (1998). "A unique model for the sand and clay behavior". In: *PROBAMAT-21<sup>st</sup> Century: Probabilities and Materials* (pp. 465-479). Springer, Netherlands. [https://doi.org/10.1007/978-94-011-5216-7\\_26](https://doi.org/10.1007/978-94-011-5216-7_26)
- Brinkgreve, R.B.J., and Vermeer, P.A. (1997). "PLAXIS finite element code for soil and rock analysis-version 7". Balkema.
- Brinkgreve, R., and Broere, W. (2006). "PLAXIS 3D foundation manual, version 1.5". Delft University of Technology and PLAXIS Bv.
- Castro, J., and Karstunen, M. (2010). "Numerical simulations of stone column installation". *Canadian Geotechnical Journal*, 47 (10), 1127-1138. <https://doi.org/10.1139/T10-019>
- Debats, J.M., Guetif, Z., and Bouassida, M. (2003). "Soft soil improvement due to vibro-compacted column installation". *Proc. Int. Workshop on Geotechnics of Soft Soils-Theory and Practice, 2000*, 551-556.
- El-Nemr, M.T., Azzam, W.R., Abu-Raia, M.M., and Wahba, M.A. (2023). "Numerical investigation of wall packing effects on geotechnical behavior of infilled frames under lateral loads". *Applications of Modeling and Simulation*, 7, 122-131.
- El Sawwaf, M., Azzam, W., Samy, A., and El Sawwaf, A. (2024). "Large-scale direct shear tests on soft clay treated with reinforced lime columns". *International Journal of Geosynthetics and Ground Engineering*, 10 (5), 85. <https://doi.org/10.1007/s40891-024-00594-8>
- El Sawwaf, M., Nazir, A., Azzam, W., and Banan, B. (2017). "Numerical study of strip footing resting on soft clay reinforced with stone columns". *International Conference on Advances in Structural and Geotechnical Engineering*, 1, 11 pages.
- Fayed, A.L., Sorour, T.M., and Shehata, H.F. (2018). "Study of the behavior of floating stone columns in soft clay formations using numerical modeling BT: Soil testing, soil stability and ground improvement". (W. Frikha, S. Varaksin, and A. Viana da Fonseca (Eds.); pp. 236-251). Springer International Publishing.
- Gibson, R.E., and Anderson, W.F. (1961). "*In-situ* measurements of soil properties with the pressuremeter". *Civ. Engrg. and Publ. Works Rev.*, 56 (658).
- Greenwood, D.A., and Kirsch, K. (1984). "Specialist ground treatment by vibratory and dynamic methods". In: *Piling and Ground Treatment* (pp. 17-45). Thomas Telford Publishing. <https://doi.org/doi:10.1680/pagt.01855.0002>
- Hadri, S., Messast, S., and Bekkouche, S. R. (2021). "Numerical analysis of the performance of stone columns used for ground improvement". *Jordan Journal of Civil Engineering*, 15 (2), 253-265.
- Hamzh, A., Mohamad, H., and Bin Yusof, M.F. (2022). "The effect of stone column geometry on soft soil bearing capacity". *International Journal of Geotechnical Engineering*, 16 (2), 200-210. <https://doi.org/10.1080/19386362.2019.1666557>
- Han, J., and Ye, S.L. (1992). "Settlement analysis of buildings on soft clays stabilized by stone columns". *Proc., Int. Conf. on Soil Improvement and Pile Found.*, 118, 446-451.
- Hight, D.W., Bond, A.J., and Legge, J.D. (1992). "Characterization of the Bothkennar clay: An overview". *Géotechnique*, 42 (2), 303-347.
- Kirsch, F. (2006). "Vibro stone column installation and its effect on ground improvement". *Proceedings of the International Conference on Numerical Simulation of Construction Processes in Geotechnical Engineering for Urban Environment, 1994*, 115-124.

- McCabe, B.A., Nimmons, G.J., and Egan, D. (2009). "A review of field performance of stone columns in soft soils". *Proceedings of the Institution of Civil Engineers: Geotechnical Engineering*, 162 (6), 323-334. <https://doi.org/10.1680/geng.2009.162.6.323>
- Mitchell, J.K., and Huber, T.R. (1985). "Performance of a stone column foundation".
- Mitra, S., and Chattopadhyay, B.C. (1999). "Stone columns and design limitations". *Proc. of Indian Geotechnical Conference, Held at Calcutta, India*, 201-205.
- Mohamed, M., Sakr, M., and Azzam, W. (2023). "Geotechnical behavior of encased stone columns in soft clay soil". *Innovative Infrastructure Solutions*, 8. <https://doi.org/10.1007/s41062-023-01044-6>
- Narasimha Rao, S., Madhiyan, M., and Prasad, Y.V.S.N. (1992). "Influence of bearing area on the behavior of stone columns". *Proceedings of the Indian Geotechnical Conference*, 235-237.
- Nash, D.F.T., Sills, G.C., and Davison, L.R. (1992). "One-dimensional consolidation testing of soft clay from Bothkennar". *Géotechnique*, 42 (2), 241-256.
- Priebe. (1995). "The design of vibro replacement. Ground engineering".
- Priebe, H.J. (1976). "Evaluation of the settlement reduction of a foundation improved by vibro-replacement". *Bautechnik*, 2, 160-162.
- Ranjan, G., and Rao, B.G. (1986). "Granular piles for ground improvement". *Proceedings of the 1<sup>st</sup> International Conference on Piling and Deep Foundations*, September, 1-5.
- Sakr, M., Azzam, W., and Sallam, M. (2022). "Performance of pile supported embankments over soft clay". *International Journal of Advances in Structural and Geotechnical Engineering*, 03 (02), 14-25. <https://doi.org/10.21608/asge.2022.152711.1010>
- Sakr, M., El Sawwaf, M., and Rabah, A. (2022a). "Numerical study of soft clay reinforced with deep cement mixing technique". *Indian Geotechnical Journal*. <https://doi.org/10.1007/s40098-022-00625-z>
- Sakr, M., El Sawwaf, M., and Rabah, A. (2022b). "Soft clay improved by deep cement mixing column technique". *Arabian Journal of Geosciences*, 15. <https://doi.org/10.1007/s12517-022-10577-6>
- Sathish, S., Yadav, O.P., and Deepak, M. (1997). "Soft ground improvement using stone columns: A field trial". *Proc. Indian Geotech. Conf*, 311-314.
- Sexton, B.G., and McCabe, B.A. (2015). "Modeling stone column installation in an elasto-viscoplastic soil". *International Journal of Geotechnical Engineering*, 9 (5), 500-512. <https://doi.org/10.1179/1939787914Y.0000000090>
- Shehata, H.F., Sorour, T.M., and Fayed, A.L. (2018). "Effect of stone column installation on soft clay behavior". *International Journal of Geotechnical Engineering*, 15 (5), 1-13. <https://doi.org/10.1080/19386362.2018.1478245>
- Vitkar, P.P. (1978). "Strip footing on weak clay stabilized with a granular trench or pile".
- Yousfi, M.A., Guettala, S., Debbabi, I.E., and Douara, T.H. (2023). "Numerical analysis of a 3D unit cell model for soft soil reinforced with different granular columns". *Jordan Journal of Civil Engineering*, 17 (4), 613-623. <https://doi.org/10.14525/JJCE.v17i4.05>